Dyes and Pigments 92 (2012) 1204–1211

Contents lists available at ScienceDirect

Dyes and Pigments

journal homepage: www.elsevier.com/locate/dyepig

Photoinduced orientational dynamics of azophenylcarbazole molecules in polycarbonate

G. Navickaitė [a], G. Seniutinas [a], R. Tomašiūnas [a,*], R. Petruškevičius [b], V. Getautis [c], M. Daškevičienė [c]

[a] Institute of Applied Research, Vilnius University, Saulėtekio 10, LT-10223 Vilnius, Lithuania
[b] Center for Physical Sciences and Technology, Savanoriu Av. 231, 02300 Vilnius, Lithuania
[c] Kaunas University of Technology, Radvilėnu pl. 19, LT-50270 Kaunas, Lithuania

ARTICLE INFO

Article history:
Received 12 February 2011
Received in revised form
29 July 2011
Accepted 1 August 2011
Available online 10 August 2011

Keywords:
Azophenylcarbazole
All-optical poling
Relaxation kinetics
Orientational diffusion
Photoinduced erasure

ABSTRACT

The synthesis and new optical features of four azophenylcarbazoles are described. All-optical poling of the azophenylcarbazoles with different donor groups was investigated. The highest optical poling efficiency ($\chi^{(2)} \simeq 0.72$ pm/V) was measured for relative larger molecules (branched). Parameters describing mobility of the azophenylcarbazoles (orientational diffusion coefficient vary from 2.2×10^{-5} s^{-1} to 8×10^{-5} s^{-1}) were extracted using an adopted model. Photoinduced erasure while reading the poled media turned out to be more pronounced for less developed structures (less branched donor). Different polymer materials were investigated as the host matrix for the most interesting azophenylcarbazole molecule.

1. Introduction

The angular redistribution of azo moieties in chromophores already attracts much attention from the interdisciplinary science community. Chemists are searching for new materials featuring original intramolecular links or diverse coupling with the surrounded matrix. Physicists look for non-linear optical properties introduced by non-centrosymmetry. Technologists have fun with profiling the films, eg. creating photoinduced surface gratings. Finally, information technologists gain from developing photofunctional devices such as optical memory and photoswitching components. The photoinduced orientation process in media containing azo junctions comprises *trans-cis-trans* photoisomerization cycles followed by a change of orientation of chromophores toward the perpendicular direction with respect to the polarized light, or in brief - angular hole burning [1]. It is well known that an all-aromatic azo chromophore has higher thermal stability than the alkyl-linked azo chromophore (eg. Disperse Red 1), which in turn informs us about improved optical stability [2]. An aromatic azo chromophore composed of an azo chromophore linked with carbazole chromophore embedded into polyimides show highly stable optically induced birefringence [3]. To gain better non-linear susceptibility crosslinking of the aligned molecules was performed [4]. Azocarbazoles with an attached epoxide ring have been immobilized via a surrounding matrix made of epoxy resin. Much potential for the optical non-linearity of carbazoles have been shown, when attaching them to multifunctional inorganic chains as polysiloxane [5] or polyphosphazene [6]. However, non-centrosymmetry of the media containing the carbazole chromophores was achieved while applying an external electric field (corona poling) [4–7]. Despite the effectiveness to align chromophores with a steady-state electric field the contactless all-optical poling method has many advantages. The quasi-phase matched condition for optical generation of harmonics (eg. second), or the measurement of the time resolved dynamics of polar media are noteworthy [8].

In this work we extend our knowledge of the non-linear optical features of azocarbazole chromophores by investigating their alignment dynamics and consequent orientational relaxation by means of the contactless all-optical poling technique. We show how the reading of polarity influences the re-orientation of the chromophores. Investigations done with different chromophores enables us to draw relationships between the embranchment of molecule and it's optical susceptibility.

* Corresponding author.
E-mail address: rolandas.tomasiunas@ff.vu.lt (R. Tomašiūnas).

0143-7208/$ – see front matter © 2011 Elsevier Ltd. All rights reserved.
doi:10.1016/j.dyepig.2011.08.004

2. Material and methods

2.1. Synthesis of chromophores

The synthetic procedure for azophenylcarbazole-based dyes **1**–**4** is summarized in Fig. 1. The synthetic strategy displays the chemical reaction scheme that was used to synthesize the key compound 3-(4-nitrophenyl)azo-9*H*-carbazol-2-ol (**1**) and is based on these concepts. Thus, azocarbazole-based dye **1** was prepared by coupling reaction of commercially available 9*H*-carbazol-2-ol (Aldrich) with a diazonium salt prepared from 4-nitroaniline. Then, the OH and NH groups of **1** were alkylated with different halogenalkanes for better solubility to yield the desired guest chromophore molecules **2**–**4**, namely 9-methyl-2-methoxy-3-(4-nitrophenyl)azo-9*H*-carbazole (**2**), 3-(4-nitrophenyl)azo-9-propyl-2-propoxy-9*H*-carbazole (**3**) and 3-(4-nitrophenyl)azo-9-(2-ethyl) hexyl-2-(2-ethyl)hexyloxy-9*H*-carbazole (**4**). All new azo dyes were identified by various spectroscopy and elemental analysis.

2.1.1. 3-(4-Nitrophenyl)azo-9H-carbazol-2-ol (**1**, $C_{18}H_{12}N_4O_3$)

4-Nitroaniline (2.07 g, 15 mmol) was dissolved in a 12% solution of HCl (13.5 mL) by heating till 50 °C. The obtained solution was cooled with an ice bath to bellow 5 °C, then an aqueous solution containing sodium nitrite (1.05 g, 65.4 mmol) was slowly added to the obtained suspension with vigorous stirring. During the addition of the solution of sodium nitrite, the temperature of the mixture was not allowed to rise above 12–15 °C. After the addition was completed the stirring was continued for about 30 min to afford a clear solution. The resulting diazonium salt solution was added with vigorous stirring to the mixture of acetone (40 mL) and ethanol (25 mL) solution of 9*H*-carbazol-2-ol (2.2 g, 12 mmol) at 0–5 °C. Then the mixture was allowed to reach room temperature and was stirred for about 4 h. The separated brownish solid was filtered off and washed with water and then with ethanol. The product was purified by recrystallization from the mixture of *THF* and 2-propanol (1:1). The azo compound **1** was obtained in 88% yield (3.5 g); m.p.: 314–315 °C (*THF*: 2-propanol, 1:1).

IR (KBr), $\bar{\nu}$, cm^{-1}: 3385 (OH, NH), 3101, 3061 (CH_{arom}), 1645 (N=N), 1518, 1340 (NO_2), 854 (CH=CH 1,4-disubstituted benzene).

^{1}H NMR (300 MHz, DMSO, δ, ppm): 12.04 (s, 1H, NH); 11.60 (s, 1H, OH); 8.54 (s, 1H, 4-H of carbazole); 8.35 (d, J = 8.8 Hz, 2H, of *p*-subst. Ph); 8.15–7.95 (m, 3H, 5-H of carbazole and *p*-subst. Ph); 7.45–7.28 (m, 2H, 7-H, 8-H of carbazole); 7.17 (t, J = 7.2 Hz, 1H, 6-H of carbazole); 6.92 (s, 1H, 1-H of carbazole).

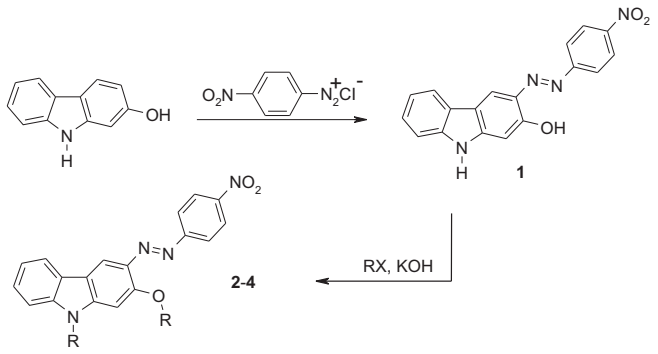

2 R = CH_3; **3** R = $CH_2CH_2CH_3$; **4** R = $CH_2CH(C_2H_5)CH_2CH_2CH_2CH_3$.

Fig. 1. Synthetic procedure of azophenylcarbazole-based dyes **1**–**4**.

Elemental analysis. Calcd. for $C_{18}H_{12}N_4O_3$ (%): C 65.06; H 3.64; N 16.86. Found (%): C 64.88; H 3.59; N 16.42.

2.1.2. 9-Methyl-2-methoxy-3-(4-nitrophenyl)azo-9H-carbazole (**2**, $C_{20}H_{16}N_4O_3$)

A mixture of azo compound **1** (1.0 g, 3.0 mmol), iodomethane (2.6 g, 18.0 mmol), 85% powdered KOH (1.2 g, 18.0 mmol), and anhydrous Na_2SO_4 (0.17 g, 1.2 mmol) was stirred at room temperature in DMF (6 mL) until the starting and monoalkylated intermediate disappeared (24 h). After termination of the reaction (TLC) the reaction mixture was extracted with ethyl acetate. The organic layer was dried ($MgSO_4$) and filtered off. Ethyl acetate and excess of iodomethane were removed under vacuum and a red solid product **2** was obtained in 74% yield (0.8 g); m.p.: 234–236 °C (recrystallized from *THF*).

IR (KBr), $\bar{\nu}$, cm^{-1}: 3045 (CH_{arom}), 2958, 2925, 2854 (CH_{aliph}), 1630 (N=N), 1515, 1335 (NO_2), 854, 745 (CH=CH 1,4- and 1,2-disubstituted benzenes).

^{1}H NMR (300 MHz, DMSO, δ, ppm): 8.50 (s, 1H, 4-H of carbazole); 8.42 (d, J = 9.0 Hz, 2H, of *p*-subst. Ph); 8.16 (d, J = 7.7 Hz 1H, 5-H of carbazole); 8.03 (d, J = 9.0 Hz, 2H, of *p*-subst. Ph); 7.60 (d, J = 7.7 Hz, 1H, 8-H of carbazole); 7.50–7.42 (m, 1H, 7-H of carbazole); 7.38 (s, 1H, 1-H of carbazole); 7.28–7.18 (m, 1H, 6-H of carbazole); 4.15 (s, 1H, OCH_3); 3.95 (s, 1H, NCH_3).

Elemental analysis. Calcd. for $C_{20}H_{16}N_4O_3$ (%): C 66.66; H 4.48; N 15.55. Found (%): C 66.38; H 4.2; N 14.92.

2.1.3. 3-(4-Nitrophenyl)azo-9-propyl-2-propoxy-9H-carbazole (**3**, $C_{24}H_{24}N_4O_3$)

Azo compound **3** was prepared according to the procedure described above for **2** except that 1-bromopropane (2.21 g, 18 mmol) instead of iodomethane was used. A red solid product **3** was obtained in 80% yield (1.0 g); m.p.: 183.5–185 °C.

IR (KBr), $\bar{\nu}$, cm^{-1}: 3045 (CH_{arom}), 2967, 2938, 2877 (CH_{aliph}), 1630 (N=N), 1515, 1324 (NO_2), 859, 740 (CH=CH 1,4- and 1,2-disubstituted benzenes).

^{1}H NMR (300 MHz, $CDCl_3$, δ, ppm): 8.53 (s, 1H, 4-H of carbazole); 8.35 (d, J = 9.0 Hz, 2H, of *p*-subst. Ph); 8.02 (d, J = 9.0 Hz, 2H, of *p*-subst. Ph); 7.49–7.34 (m, 2H, 8-H, 7-H of carbazole); 7.28–7.21 (m, 1H, 6-H of carbazole); 6.90 (s, 1H, 1-H of carbazole); 4.42–4.12 (m, 4H, OCH_2, NCH_2); 2.18–1.85 (m, 4H, CH_2CH_3); 1.18 (t, J = 7.4 Hz, 3H, CH_3); 1.03 (t, J = 7.4 Hz, CH_3).

Elemental analysis. Calcd. for $C_{24}H_{24}N_4O_3$ (%): C 69.21; H 5.81; N 13.45. Found (%): C 69.08; H 5.62; N 13.04.

2.1.4. 3-(4-Nitrophenyl)azo-9-(2-ethyl)hexyl-2-(2-ethyl)hexyloxy-9H-carbazole (**4**, $C_{34}H_{44}N_4O_3$)

Azo compound **4** was prepared according to the procedure described above for **2** except that 2-ethylhexylbromide (3.51 g, 18 mmol) instead of iodomethane was used. Product **4** was purified by column chromatography (eluent: acetone:*n*-hexane = 1:24). Yield of **4** was 1.2 g (75%); m.p.: 76.5–78 °C (acetone:ethanol, 1:1).

IR (KBr), $\bar{\nu}$, cm^{-1}: 3068 (CH_{arom}), 2958, 2925, 2872, 2857 (CH_{aliph}), 1628 (N=N), 1521, 1322 (NO_2), 857, 743 (CH=CH 1,4- and 1,2-disubstituted benzenes).

^{1}H NMR (300 MHz, $CDCl_3$, δ, ppm): 8.45 (s, 1H, 4-H of carbazole); 8.37 (d, J = 8.9 Hz, 2H, of *p*-subst. Ph); 7.98 (d, J = 8.9 Hz, 2H, of *p*-subst. Ph); 7.58–7.32 (m, 2H, 8-H, 7-H of carbazole); 7.31–7.11 (m, 2H, 1-H, 6-H of carbazole); 4.41–4.06 (m, 4H, OCH_2, NCH_2); 2.11–1.75 (m, 2H, CH); 1.65–1.06 (m, 16H, $CH(CH_2)CH_2CH_2CH_2CH_3$); 1.03–0.68 (m, 12H, CH_3).

Elemental analysis. Calcd. for $C_{34}H_{44}N_4O_3$ (%): C 73.35; H 7.97; N 10.06. Found (%): C 73.08; H 7.62; N 9.64.

2.2. Characterization of chromophores

^{1}H NMR spectra were measured on a *Varian Unity Inova* spectrometer (300 MHz) in DMSO-d_6 or $CDCl_3$. The IR spectra of the samples in KBr pellets were recorded on a *Perkin Elmer Spectrum GX FT-IR System* spectrometer. The absorption spectra of the sample THF solutions (10^{-4} M) placed in a 1 mm path length microcell were recorded on a *Perkin Elmer Lambda 35 UV/VIS* spectrometer. The course of the reactions was monitored by TLC on *Merck TLC* aluminum Silica gel 60 F_{254} sheets and developed with UV light. Silica gel (grade 62, 60–200 mesh, 150 Å, *Aldrich*) was used for column chromatography. Elemental analyses were performed with an Exeter Analytical CE-440 Elemental Analyzer. Melting points were determined in capillary tubes on capillary melting point apparatus *Electrothermal MEL-TEMP®*. Optical characterization via measuring optical absorption spectra of the films was performed using dual beam spectrophotometer *Shimadzu UV-3101PC* (Fig. 2).

2.3. Preparation of films

The four different azophenylcarbazoles **1**–**4** (Fig. 3) were dispersed in a polycarbonate matrix for optical poling experiments. The samples were prepared by a spin-coating technique involving a 500 cycles per min spin for the first 6 s followed by a 2000 cycles per min spin for the next 20 s. Silica glass plates were used as substrates and were degreased in ethanol, washed in distilled water and dried. Polycarbonate *Iupilon Z-200* with $T_g = 189$ °C was chosen as the polymer matrix for these molecules to create guest-host system.

In order to avoid aggregation, the loading density of chromophores in all samples was chosen as 10% (wt%). Drying via two steps (25 min at room temperature followed up by 45 min at 80 °C) was performed for finishing.

2.4. Technique for optical poling

The all-optical poling technique permits polar orientation of molecules. If the material with the initial centrosymmetry of the structure is irradiated with fundamental ω and its second harmonic 2ω beams it is able to absorb these beams, quantum interference between two photons of fundamental and one photon of the second harmonic to the same energy level can be achieved. The coherent pumping of the NLO polymer film results in an orientational hole burning [8,9]. Thus, provided there is a phase difference between these seeding beams, a poling electric field inside the material results. The orientational hole burning is followed by a reversible *trans-cis-trans* isomerization process, which drives optical orientation motion. Finally, it leads to a net permanent molecular polar order. This induced molecular orientation breaks the initial centrosymmetry of the structure inside the material creating a quasi-phase-matched grating of non-linear second-order susceptibility applicable to the second harmonic generation. The highest poling yield is achieved when polarization of the seeding beams is both linear and parallel and the probability of the material to absorb 1 photon of second harmonic frequency and two photons of fundamental frequency is the same [8]. We used a two-branch experimental setup [10]. The light source was a Nd:YAG laser (1064 nm, 20 ns, 10 Hz). From the two branches frequency doubled (2ω) and first harmonic ω beams served as seeding beams. These two beams of Gaussian profile were focused on the sample at the same spot of 200 μm diameter. A pair of shutters was used to alter the seeding and probing processes. Optically induced second-order susceptibility of the sample was measured via second harmonic generation of the ω beam. During the reading process the 2ω beam was blocked and only the ω beam was left, so its energy and spot size were the same as during the seeding period. The decay of second harmonic generation was measured either using permanent pulsed irradiation by the reading beam ("light"), or not permanent pulsed irradiation ("dark"), when probing was performed by measuring a few single laser shots only, thus, having minimal influence on the decay process from the reading beam. No photothermal heating of samples was observed because of low loading density of chromophores and relatively high glass transition temperature for the polycarbonate polymer matrix used.

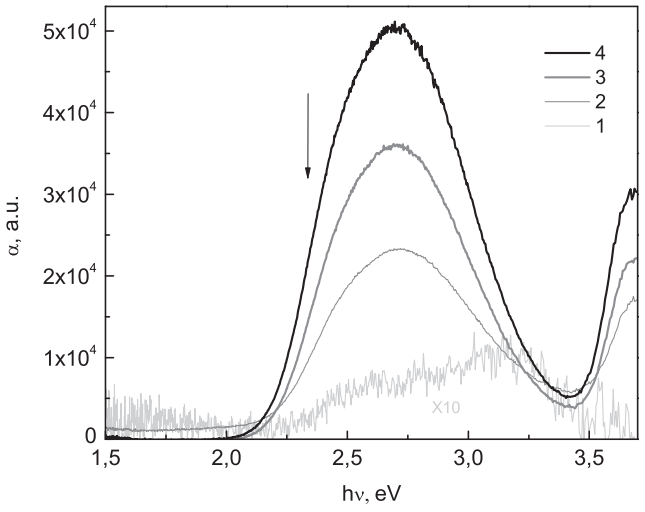

Fig. 2. Spectral dependence of absorption coefficient α for azophenylcarbazole samples. Arrow indicates quantum energy (2.34 eV) for the second harmonic light.

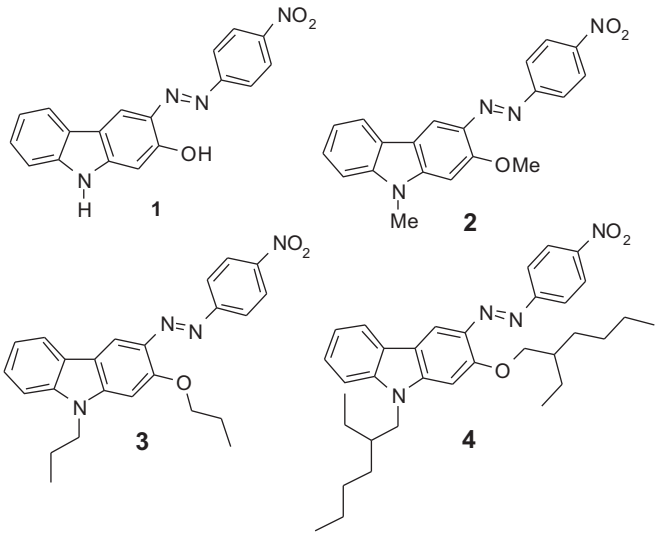

Fig. 3. Molecular structure of azophenylcarbazole samples.

3. Theory and calculation

The physical origin of all-optical poling is attributed to orientational hole burning and molecular re-orientation of azo-dye chromophores in a polymer host matrix. This process can be described by two coupled orientational diffusion equations for

photoexcitation and re-orientation of azo-dye molecules in *trans* and *cis* states [11,14,15]:

$$\begin{cases} \dfrac{\partial n_t(\Omega)}{\partial t} &= -\xi I(\theta) n_t(\Omega) + \phi \int\int \Phi(\Omega' \to \Omega) I(\theta') n_c(\Omega') d\Omega' + \dfrac{1}{\tau_c} \int\int G(\Omega' \to \Omega) n_c(\Omega') d\Omega' + D_t \nabla^2 n_t(\Omega) \\ \dfrac{\partial n_c(\Omega)}{\partial t} &= -\phi I(\theta) n_c(\Omega) + \xi \int\int Q(\Omega' \to \Omega) I(\theta') n_t(\Omega') d\Omega' - \dfrac{1}{\tau_c} n_c(\Omega) + D_c \nabla^2 n_c(\Omega) \end{cases}, \quad (1)$$

where $n_t(\Omega)$ and $n_c(\Omega)$ are the molecular density of *trans* and *cis* isomers, respectively, with dipole momentum direction in the solid angle $\Omega(\theta, \phi)$. ξ and ϕ are the quantum efficiency of *trans*-to-*cis* and *cis*-to-*trans* photoisomerization, respectively. τ_c represents the lifetime of *cis* isomer defined by thermal relaxation rate. $G(\Omega' \to \Omega)$ is the probability for molecules to rotate from Ω' to Ω in the process of *cis*-to-*trans* thermal recovery. $Q(\Omega' \to \Omega)$ and $\Phi(\Omega' \to \Omega)$ are probabilities of *trans*-to-*cis* and *cis*-to-*trans* optical transition, respectively. D_t and D_c are thermal-induced orientational diffusion constants for *trans* and *cis* isomers, respectively.

The first term in Eq. (2) (upper) and the second term in Eq. (2) (lower) define isomerization of *trans* to *cis* state under photoexcitation. Isomerization of *cis* to *trans* state describe the first term in Eq. (2) (lower) and the second term in Eq. (2) (upper). The third and the forth terms stand for thermal-induced relaxation of *cis* isomer back to *trans* state and for molecular orientational diffusion, respectively. Further, we neglect the term $I(\theta)n_c(\Omega)$ by setting $\phi = 0$, because the orientational hole burning mechanism for the ball-like *cis* isomer molecules is less important [1]. Thus, Eq. (2) simplifies into:

$$\begin{cases} \dfrac{\partial n_t(\Omega)}{\partial t} = -\xi I(\theta) n_t(\Omega) + \dfrac{1}{\tau_c} \int\int G(\Omega' \to \Omega) n_c(\Omega') d\Omega' + D_t \nabla^2 n_t(\Omega) \\ \dfrac{\partial n_c(\Omega)}{\partial t} = \xi \int\int Q(\Omega \to \Omega) I(\theta') n_t(\Omega') d\Omega' - \dfrac{1}{\tau_c} n_c(\Omega) + D_c \nabla^2 n_c(\Omega) \end{cases}, \quad (2)$$

what would correspond to a transition scheme depicted in Fig. 4.

The orientational hole burning mechanism for *trans* isomer in all-optical poling is represented by the term $I(\theta)n_t(\Omega)$, where $I(\theta)$ is azo-dye excitation rate:

$$I(\theta) = I_1 \cos^2\theta + I_2 \cos^4\theta + I_3 \cos^3\theta, \quad (3)$$

with

$$I_1 \alpha \mu_{01}^2 \left| E_{2\omega}^2 \right|,$$
$$I_2 \alpha \frac{\mu_{01}^2 \Delta\mu^2}{(2\hbar\omega)^2} \left| E_{\omega}^4 \right|,$$
$$I_3 \alpha \frac{\mu_{01}^2 \Delta\mu}{\hbar\omega} \left| E_{\omega}^2 E_{2\omega}^* \cos(\Delta\Psi + \Delta kz) \right|,$$

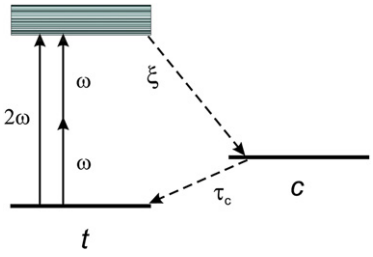

Fig. 4. Scheme of transitions.

where μ_{01} is the transition dipole moment and $\Delta\mu = \mu_1 - \mu_0$ is the difference between the dipole moments in the excited and ground state for two-level molecule approximation of rod-like azo-dye chromophore [8]. Parameters I_1, I_2, I_3 correspond respectively to excitation terms of one-photon absorption at frequency 2ω (field amplitude $E_{2\omega}$), two-photon absorption at frequency ω (field amplitude E_ω) and the interference between these two terms. $\Delta\Psi$ corresponds to the phase difference between two beams on the incident surface of the sample. $(\Delta\Psi + \Delta kz)$ is the relative phase between two beams after propagation over distance z. The term containing $I_3\cos^3\theta$ bears polarity, which is the origin of photoinduced polar orientation [8,9].

In a simple case of rod-like molecules of the *trans* isomer and the ball-like molecules of the *cis* isomer excited with linear polarization of the seeding beams at frequencies ω and 2ω, the all-optical poling process preserves symmetry around the polarization direction. As a consequence, the angular distributions $n_t(\Omega)$ and $n_c(\Omega)$ depend only on the polar angle θ and can be projected on Legendre polynomials $P_j(\cos\theta)$ by introducing expansion coefficients T_j and C_j called the Order Parameters for *trans* and *cis* isomers [11,15]:

$$n_t(\Omega) = n_t(\theta) = \frac{1}{2\pi} \sum_{j=0}^{\infty} \frac{2j+1}{2} T_j P_j(\cos\theta), \quad (4)$$

$$n_c(\Omega) = n_c(\theta) = \frac{1}{2\pi} \sum_{j=0}^{\infty} \frac{2j+1}{2} C_j P_j(\cos\theta), \quad (5)$$

The probabilities of redistribution processes $G(\Omega' \to \Omega)$ and $Q(\Omega' \to \Omega)$ depend only on the rotation angle χ between directions Ω' and Ω, therefore we can expand them in terms of the Legendre polynomials $P_j(\cos\chi)$ as well [11,15].

$$G(\Omega' \to \Omega) = G(\chi) = \frac{1}{2\pi} \sum_{m=0}^{\infty} \frac{2m+1}{2} G_m P_m(\cos\chi), \quad (6)$$

$$Q(\Omega' \to \Omega) = Q(\chi) = \frac{1}{2\pi} \sum_{k=0}^{\infty} \frac{2k+1}{2} Q_k P_k(\cos\chi), \quad (7)$$

where G_m and Q_k describe the shape of probability functions.

In the case of an assembly of non-interacting molecules, the macroscopic polarizability can be theoretically obtained from the corresponding microscopic polarizability β after averaging over all possible orientations, that is,

$$\chi^{(2)} = \int n(\Omega) \beta d\Omega, \quad (8)$$

where $n(\Omega)$ is the molecular density oriented in the solid angle Ω. Considering the azo-dye polymeric system dominated by rod-like molecules of *trans* isomer, the induced $\chi^{(2)}$ can be expressed in terms of the *trans* isomer order parameters T_j [11,14,15].

For the first time to our knowledge Eq. (2) is converted into a system of 10 ordinary differential equations for Order Parameters T_0, T_1, T_2, T_3, T_4 of *trans* and C_0, C_1, C_2, C_3, C_4 of *cis* isomers, respectively, using Eqs. (4)–(7) for sets of orthogonal Legendre

polynomials up to the fourth order. The system was solved using Matlab software for the CW (continuous wave) excitation case. It was assumed that before poling process starts all azo-dye molecules are in *trans* isomer state and oriented isotropically. Initial values of parameters required for numerical simulation were chosen close to real ones obtained in our previous experiments with azo-dye doped polymer materials [10]. The quantum efficiency of *trans*-to-*cis* photoisomerization $\xi = 0.11$ was taken from the literature [14]. It was assumed that orientational diffusion coefficients for the *trans* and *cis* isomer D_t and D_c, respectively, are equal. Initial values for expansion parameters of probability function $G_1 = Q_1 = 0.85$, $G_2 = Q_2 = 0.61$, $G_3 = Q_3 = 0.38$, $G_4 = Q_4 = 0.21$, are defined by Boltzman-like probability distribution and similar to ones obtained in literature [16].

4. Results

Four different azophenylcarbazole-based chromophores in a polycarbonate matrix were investigated, though only three of them (**2**, **3** and **4**) showed an optical poling effect. No measurable second harmonic signal was obtained for chromophore **1** (donor termination by H and OH). Poling graphs for the three samples using the same excitation condition (pulse energy) for seeding and reading are shown in Fig. 5. Independently from the embranchment of molecules poling proceeds in a quite similar way and reaches saturation after ~10 min. The saturation informs us about some quasi-stationary situation, when the balance between poling and depoling processes occurs, i.e. *trans*-to-*cis* transition rate approaches the decay rate of poled media defined by re-orientational diffusion of molecules in the *trans* and *cis* states, thermal and photoinduced *cis*-to-*trans* transition. The efficiency to generate a second harmonic strongly differs and depends on the embranchment of molecules as expected. The highest value for the most branched chromophore **4** obtained may be explained by larger partial volume and dipole moment of the molecule considering higher polarizability. For the smallest chromophore **1** the polarizability was probably too low to detect a second harmonic signal. Reabsorption of the second harmonic radiation shouldn't be considered since the poling efficiency goes in the opposite direction as the absorbance at 2.34 eV for chromophores investigated (see Fig. 2).

After poling is stopped, a domain characterized by relatively fast relaxation occurs, which could relate to thermal back-reaction of *cis*-to-*trans* isomerization, and is common for all chromophores measured (see Fig. 6). The much slower second time domain concerns mainly the loss of induced polar order by thermal-induced orientational diffusion [2]. The complexity of the process people describe via multi-exponential decay [11]. In our case the difference in the slow part of the kinetics is obvious, what features longer lasting poled media with more branched chromophores.

To investigate the density of molecules in the *trans* state, measurements at different seeding energies were performed. Basically no difference in the magnitude of the signal was obtained, when reading the poled media with the same energy beam (Figs. 7 and 9). It indicates that almost all the molecules in the *trans* state available for excitation have performed *trans*-to-*cis* transition even for the lowest energy of the seeding beam applied (curves c). The result shows that depletion of molecules in the *trans* states is achievable for chromophores of different embranchment (samples **4** and **2**). The dynamic poled media loses it's orientation does not greatly depend upon the embranchment, however, some deviation to faster decay appears for the smaller chromophore (sample **2**) under the highest excitation condition $I_\omega = 2.8$ J/cm^2, $I_{2\omega} = 0.45$ mJ/cm^2, what may refer to increased flexibility due to heating the media (compare Figs. 8 and 10).

Photoinduced orientational relaxation of the poled media was investigated by measuring the decay in "light" and "dark" regimes. The reading beam induces more rapid decay, i.e. effective "washing-out" of the orientation alignment of molecules (Figs. 11–13) for all chromophores investigated.

To evaluate the macroscopic second-order optical non-linearity of the material a comparison of second-order non-linear susceptibility $\chi^{(2)}$ between azophenylcarbazole and *z*-cut quartz plate was performed using equation [12]:

$$\frac{\chi^{(2)}}{\chi_q^{(2)}} = \frac{2}{\pi}\frac{l_{c,q}}{d}\sqrt{\frac{I^{2\omega}}{I_q^{2\omega}}}, \tag{9}$$

where the coherence length $l_{c,q} = \lambda_\omega/(4(n_{q(2\omega)} - n_{q(\omega)}))$ and the refractive index n are parameters for quartz and d is the thickness of the azophenylcarbazole film. ω and 2ω denote the fundamental and the second harmonic beam. $I^{2\omega}$ and $I_q^{2\omega}$ are the second harmonic

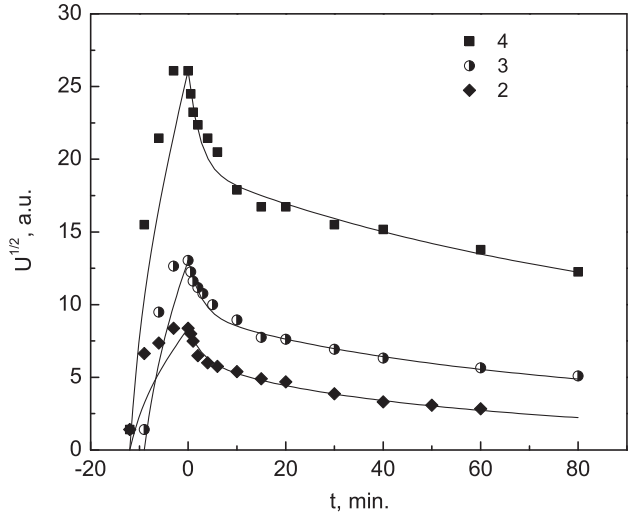

Fig. 5. Second harmonic radiation generated by optically poled azophenylcarbazole of different embranchment (seeding beam: $I_{1\omega}$ - 1.82 J/cm^2, $I_{2\omega}$ - 0.16 mJ/cm^2; reading beam: $I_{1\omega}$ - 1.82 J/cm^2) ("dark" regime for reading process). Lines are modeling results according Eq. (2) explained in Section 3.

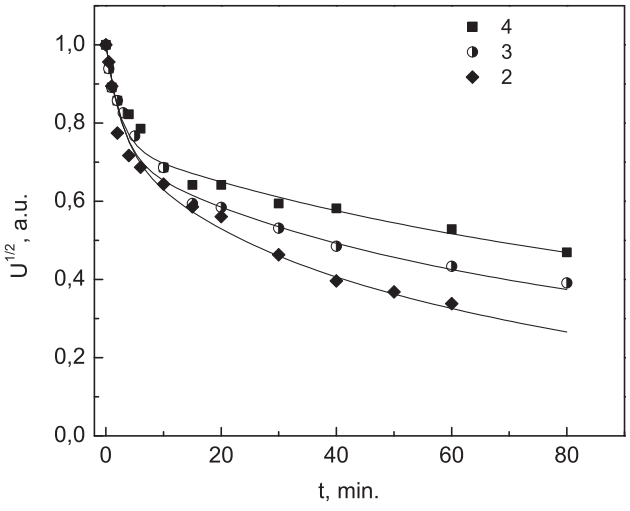

Fig. 6. Decay of second harmonic radiation generated by optically poled azophenylcarbazole of different embranchment (seeding beam: $I_{1\omega}$ - 1.82 J/cm^2, $I_{2\omega}$ - 0.16 mJ/cm^2; reading beam: $I_{1\omega}$ - 1.82 J/cm^2) ("dark" regime for reading process) (normalized signal). Lines are modeling results according Eq. (2) explained in Section 3.

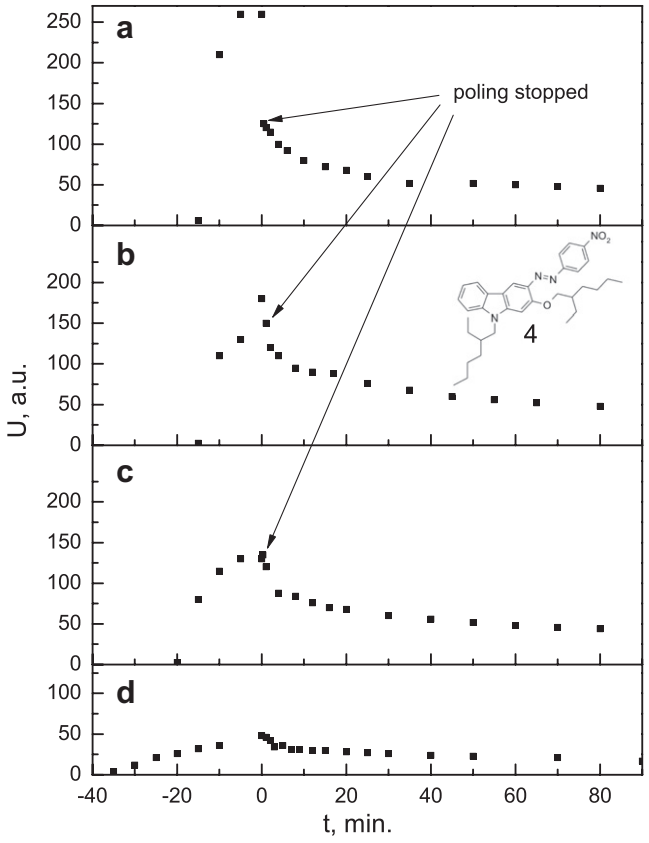

Fig. 7. Second harmonic radiation generated by optically poled azophenylcarbazole sample **4** for different seeding beam values: a) $I_{1\omega}$ - 2.8 J/cm^2, $I_{2\omega}$ - 1.4 mJ/cm^2; b) $I_{1\omega}$ - 1.82 J/cm^2, $I_{2\omega}$ - 1.2 mJ/cm^2; c) $I_{1\omega}$ - 1.5 J/cm^2, $I_{2\omega}$ - 0.9 mJ/cm^2; d) illustration of non-optimal beam polarization case, conditions same as b) (reading beam: $I_{1\omega}$ - 1.8 J/cm^2) ("dark" regime for reading process).

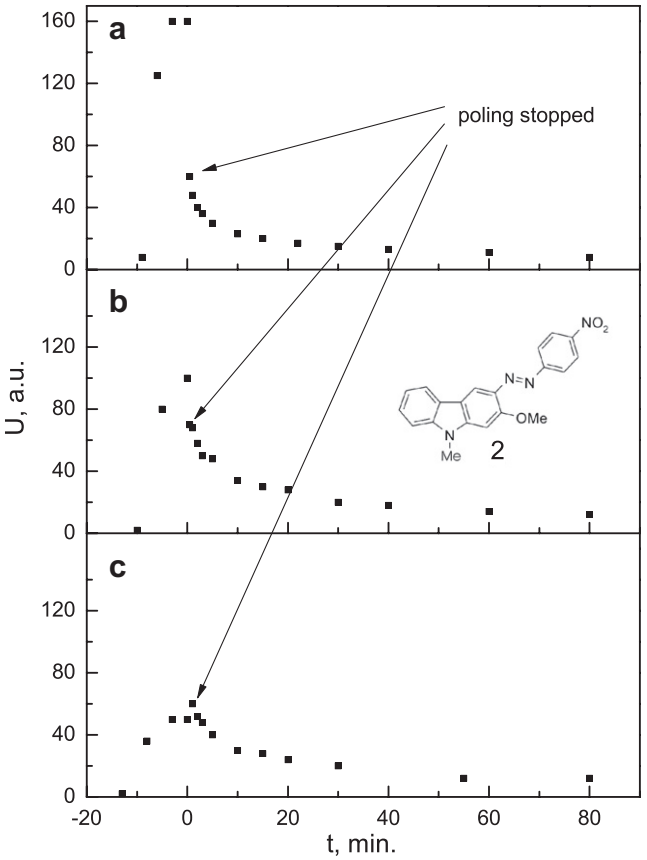

Fig. 9. Second harmonic radiation generated by optically poled azophenylcarbazole sample **2** for different seeding beam values: a) $I_{1\omega}$ - 2.8 J/cm^2, $I_{2\omega}$ - 0.45 mJ/cm^2; b) $I_{1\omega}$ - 1.82 J/cm^2, $I_{2\omega}$ - 0.16 mJ/cm^2; c) $I_{1\omega}$ - 1.5 J/cm^2, $I_{2\omega}$ - 0.1 mJ/cm^2; (reading beam: $I_{1\omega}$ - 1.82 J/cm^2) ("dark" regime for reading process).

intensities measured from azophenylcarbazole film and quartz plate, respectively. The values of $\chi_q^{(2)}$ for quartz measured over the past two decades had a wide range from 1.0 to 0.6 pm/V [13]. The latter value claimed as more accurate was used in our calculation for *z*-cut quartz plate. For sample **4** (film thickness 1.5 μm measured using AFM) best featuring optical poling the obtained $\chi^{(2)} \simeq 0.72$ pm/V is only slightly higher than that of *z*-cut quartz.

The theoretical model developed was used to extract parameters for azophenylcarbazole material via best fit of the experimental data. It's important to note that comparison between "dark" and "light"

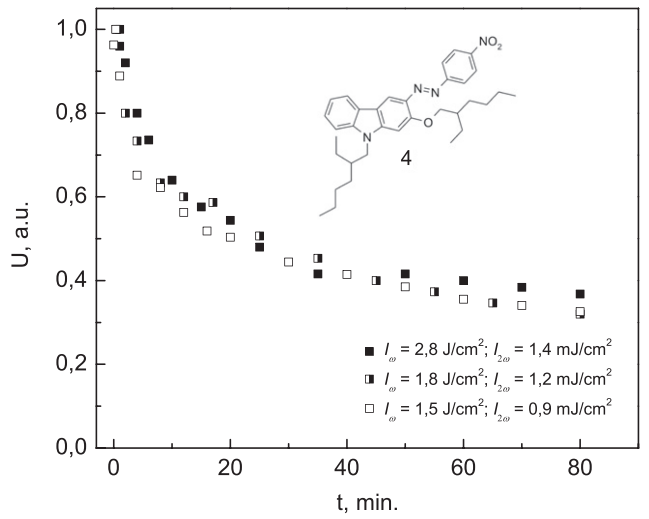

Fig. 8. Decay of second harmonic radiation generated by optically poled azophenylcarbazole sample **4** for different seeding beam values (reading beam: $I_{1\omega}$ - 1.8 J/cm^2) ("dark" regime for reading process) (normalized signal).

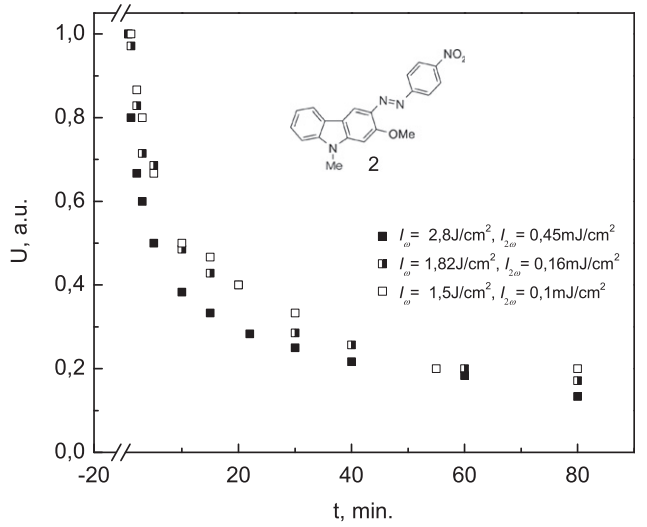

Fig. 10. Decay of second harmonic radiation generated by optically poled azophenylcarbazole sample **2** for different seeding beam values (reading beam: $I_{1\omega}$ - 1.82 J/cm^2) ("dark" regime for reading process) (normalized signal).

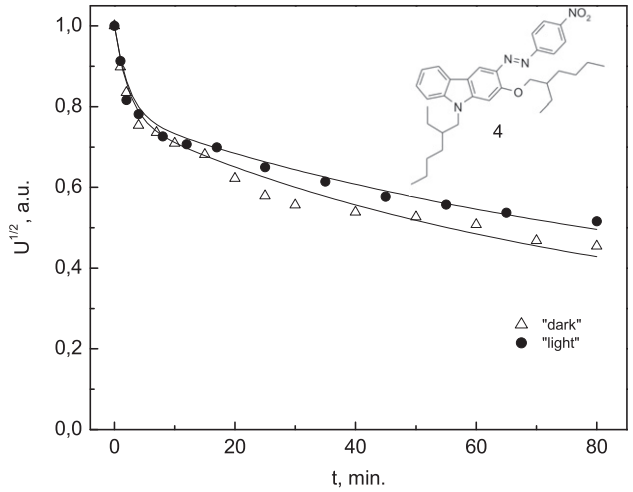

Fig. 11. Decay of second harmonic radiation generated by optically poled azophenylcarbazole sample **4** for different reading regimes ("dark" and "light") (seeding beam: $I_{1\omega}$ - 1.8 J/cm^2, $I_{2\omega}$ - 1.4 mJ/cm^2; reading beam: $I_{1\omega}$ - 1.8 J/cm^2) (normalized signal). Lines are modeling results according Eq. (2) explained in Section 3.

reading regimes allowed us to evaluate relative one- and two-photon excitation rates for these carbazole based chromophores in polycarbonate. Parameters obtained from fitting the data in Figs. 11–13 are presented in Table 1. The same parameters also align well with the poling kinetics measured using a larger pulse energy ratio between seeding beams (see Figs. 5 and 6). We obtained the relationship that the larger the chromophore size (material 4) the smaller the value of it's orientational diffusion coefficient D_t.

To investigate how thermal-induced orientational diffusion of azophenylcarbazole chromophores and the *trans*-to-*cis* photoisomerization are dependent on the guest-host system and whether it is possible to fix better the poled media created in polycarbonate, different polymer host matrices were used. By use of photopolymerization of organically modified silica (ormosil) and commercially available inorganic-organic hybrid polymers (ORMOCER) it should be possible to fix the oriented media. Experiments were performed with chromophore **4** which showed the greatest optical poling in polycarbonate. However, without a success; no signal indicating poling condition in the matrices was obtained.

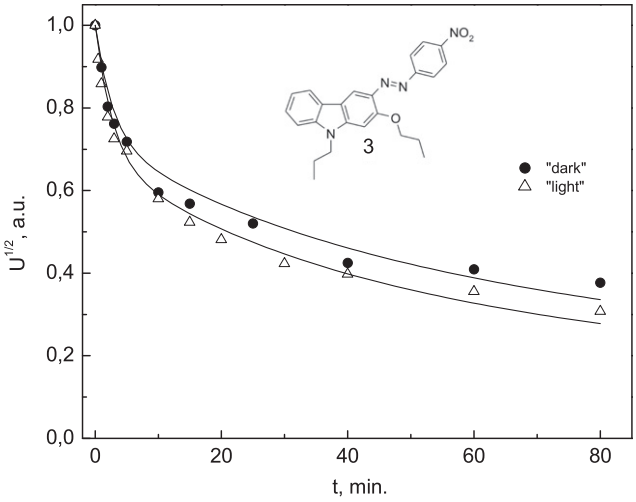

Fig. 12. Decay of second harmonic radiation generated by optically poled azophenylcarbazole sample **3** for different reading regimes ("dark" and "light") (seeding beam: $I_{1\omega}$ - 1.8 J/cm^2, $I_{2\omega}$ - 1.1 mJ/cm^2; reading beam: $I_{1\omega}$ - 1.8 J/cm^2) (normalized signal). Lines are modeling results according Eq. (2) explained in Section 3.

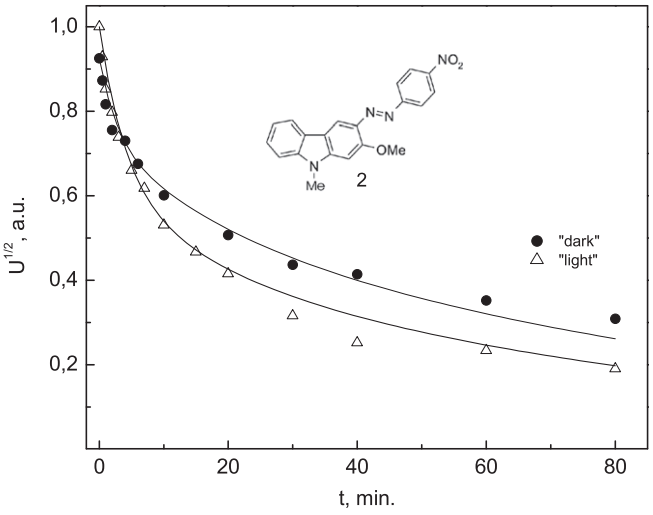

Fig. 13. Decay of second harmonic radiation generated by optically poled azophenylcarbazole sample **2** for different reading regimes ("dark" and "light") (seeding beam: $I_{1\omega}$ - 1.8 J/cm^2, $I_{2\omega}$ - 1.4 mJ/cm^2; reading beam: $I_{1\omega}$ - 1.8 J/cm^2) (normalized signal). Lines are modeling results according Eq. (2) explained in Section 3.

Probably, too rapid orientational diffusion and back-reaction of *cis*-to-*trans* isomerization in the relative fluid substance has defined the very fast decay of poled media. Following this disappointing result the search for new host matrices are in progress.

5. Discussion

Experimental investigation revealed accordance between the strength of optical absorbance and efficiency of optical poling for azophenylcarbazoles in polycarbonate with the most significant effect noted for the chromophore with the highest branched donor (see Figs. 2 and 5).

The experiment and theoretical modeling disclose polar order relaxation kinetics of carbazoles roughly split into two time periods, short and long. The long term period (over 30 min) is fully characterized by only *trans* isomer orientational diffusion coefficient D_t and this coincides well with previous data [8,10,11]. For the short time period (up to 30 min) the relaxation kinetics of polar order is defined by many parameters of the azo-polymer system. First of all, the importance of the parameters G_m and Q_k standing for probabilities of redistribution process, which was mainly not noted in previous works. In Ref. [8], it was assumed that $G(\Omega' \rightarrow \Omega) = 1/4\pi$ and $G_0 = 1$, $G_1 = G_2 = G_3 = G_4 = 0$. This implies that after excitation, each chromophore may rotate from its initial direction by any angle in any azimuthal direction and with the same probability. In Refs. [11,15], it was assumed that $G_1 \times Q_1 << 1$ and all expansion coefficients are small and does not influence the relaxation kinetics. Rather strong influence on the fitting procedure for the short time scale was observed, when the finite values of G_m and Q_k were taken into account. Thus, the G_m values obtained demonstrate the *trans*-to-*cis* thermal recovery input in orientational rotation, however, without significant difference for our samples.

Table 1
Parameters used for modeling the experimental optical poling kinetics for "light" and "dark" reading regimes of azocarbazole chromophores dispersed in polycarbonate.

Material	I_1 (s^{-1})	I_2 (s^{-1})	G_1	D_t (s^{-1})	D_c (s^{-1})	τ_c (s)
4	4×10^{-5}	2×10^{-3}	0.85	2.2×10^{-5}	2.2×10^{-5}	143
3	4×10^{-5}	2×10^{-3}	0.8	4×10^{-5}	4×10^{-5}	167
2	4×10^{-5}	1×10^{-3}	0.85	8×10^{-5}	8×10^{-5}	167

It is defined that the read-out of a poled structure by a high intensity fundamental wave induces additional decay of the recorded micro-pattern. The physics behind rests on different excitation condition while seeding or reading. At the time of reading using one beam (ω) no resulting poled electric field is provided. Alternating electric field via hole burning affects all the molecules, independently of their transition dipole moment orientation, including those responsible for the poled media and quasi-phase matched condition, thus, stimulating the erasure effect. From the modeling point of view it appears via the second term in Eq. (3), experimentally - from Figs. 11–13.

Another important fact revealed concerns the relaxation kinetic dependence on the history of seeding process. There is some "memory" effect related to seeding conditions, i.e. the pulse energy (first and second harmonic) and the seeding time. For different seeding conditions we obtain different relaxation kinetics of polar order (see Fig. 8). This fact could be interpreted using our all-optical poling model for *trans* and *cis* isomer components. The generated density of *cis* isomer component, which strongly depends on seeding conditions, even in full "dark" free relaxation regime has a back-reaction to *trans* isomer. *Cis* to *trans* thermal relaxation created an additional source of polar order for *trans* isomer and this process changes considerably the decay kinetic. The short term relaxation time starts to depend on generated density of the *cis* isomer, meanwhile the long term relaxation time of polar order is defined only by orientational diffusion constant of the *trans* isomer. This process is described by second term in Eq. (2).

In comparison to other dyes azophenylcarbazoles show relative low value of second-order non-linear susceptibility $\chi^{(2)}$. Several aspects are important to explain. The $\chi^{(2)}$ basically depends on two parameters: the molar concentration and the first-order hyperpolarizability (Eq. (8)). The molar concentration we used (10% (wt %)) corresponds well to the mid of range used for carbazoles (2% - [17], 5% - [4], 10% - [6], 38% - [18] depending on host material). From the quantum-mechanical two-level model following expression for the first-order hyperpolarizability is valid [19]:

$$\beta = \frac{2\pi^2 \Delta\mu(\mu_{eg}^2)}{\varepsilon_0 h^2} \frac{3\omega_{eg}^2}{(\omega_{eg}^2 - 4\omega^2)(\omega_{eg}^2 - \omega^2)}, \qquad (10)$$

where $\Delta\mu = \mu_e - \mu_g$ is the difference between the excited and ground state dipole moment, μ_{eg} is the transition dipole moment between the ground and excited state, ε_0 is the vacuum permittivity and ω_{eg} is the transition frequency. μ_{eg} is related to the overall strength of the transition and according to general quantum mechanics can be determined from the area under absorption band. This is quite well represented in our case for azophenylcarbazoles: the ten times difference in effect of optical poling could be attributed to the strength of transition, what basically depends on donor architecture (Figs. 2 and 5). It is most probable that both, the dipole moment and the transition dipole moment, are responsible for the relative low $\chi^{(2)}$. Same for the screening effect provided by photoinduced *cis* isomer with typically strong donor–acceptor interaction, which affects (lowers) the non-centrosymmetry of the optically poled material. It is worth emphasizing that all-optical poling revealed azophenylcarbazole as material suitable for studying molecule orientation dynamics, other photoinduced phenomena and having potential in application for optical storage.

6. Conclusions

The ability of azophenylcarbazoles to create a media featuring non-centrosymmetry was demonstrated. All-optical poling investigations revealed that the architecture of molecules (different donor) defines their orientational mobility. Thus, the larger the chromophore the weaker the orientational diffusion (diffusion coefficient vary from 2.2×10^{-5} s^{-1} to 8×10^{-5} s^{-1}) was obtained. The highest optical poling efficiency was measured for large molecules, however, photoinduced erasure while reading the poled media was more pronounced for less developed structures (weakly branched donor). The second-order non-linear optical susceptibility for azophenylcarbazoles evaluated ranges to $\chi^{(2)} \simeq 0.72$ pm/V. Modeling revealed that expansion parameters up to the fourth order for probability functions of redistribution process for both *trans* and *cis* states have to be taken into account, when interpreting the experimental results. Among different polymer matrices investigated only polycarbonate kept azocarbazole molecules relatively oriented.

Acknowledgments

This work was partially funded by a grant (No. AUT-06/2010) from the Research Council of Lithuania, by a grant from the Lithuanian State Science and Studies Foundation (project Mulatas 2), by the Agency of International Science and Technology Development in Lithuania and by the EU COST Action MP0702, MP0604. The authors wish to express their appreciation to G.Medeišienė for sample preparation and L.Kučinskaitė for numerical simulations.

References

[1] Sekkat Z, Dumont M. Photoinduced orientation of azo dyes in polymeric films - characterization of molecular angular mobility. Synth Met 1993;54:373–81.
[2] Verbiest T, Burland DM, Jurich MC, Lee VY, Miller RD, Volksen W. Exceptionally thermally stable polyimides for 2nd-order nonlinear-optical applications. Science 1995;268:1604–6.
[3] Chen JP, Labarthet FL, Natansohn A, Rochon P. Highly stable optically induced birefringence and holographic surface gratings on a new azocarbazole-based polyimide. Macromolecules 1999;32:8572–9.
[4] Niziol J, Pielichowski J. Usability of epoxy resins in conjunction with carbazole dyes in non-linear optics applications. Opt Mater 2010;32:673–6.
[5] Li J, Qin JG, Ye C. Three series of multifunctional polysiloxane attached with charge-transporting agents and electro-optical chromophores. Synth Met 2005;152:305–8.
[6] Zhang L, Huang MM, Jiang ZW, Yang Z, Chen ZJ, Gong QH, et al. A carbazole-based photorefractive polyphosphazene prepared via post-azo-coupling reaction. React Funct Polym 2006;66:1404–10.
[7] Qin Z, Fang C, Pan Q, Gu Q, Chen F, Li F, et al. Optical properties of NAEC-PMMA nonlinear polymeric thin film. J Mater Sci 2002;37:4849–52.
[8] Fiorini C, Charra F, Nunzi JM, Raimond P. Quasi-permanent all-optical encoding of noncentrosymmetry in azo-dye polymers. J Opt Soc Am B 1997;14:1984–2003.
[9] Dumont M. Dynamics of all-optical poling of photoisomerizable molecules. I. Symmetries of tensorial properties. J Opt Soc Am B 2009;26:1057–75.
[10] Seniutinas G, Laipniece L, Kreicberga J, Kampars V, Gražulevičius J, Petruškevičius R, et al. Orientational relaxation of three different dendrimers in polycarbonate matrix investigated by optical poling. J Opt A Pure Appl Opt 2009;11:034003.
[11] Liu X, Xu G, Si J, Ye P, Li Z, Shen Y. Erasure effect of the reading beam on the decay process of $\chi^{(2)}$ in all-optical poling. Appl Phys B 2000;71:539–43.
[12] Sahraoui B, Luc J, Meghea A, Czaplicki R, Fillaut JL, Migalska-Zalas A. Nonlinear optics and surface relief gratings in alkynyl–ruthenium complexes. J Opt A Pure Appl Opt 2009;11:024005.
[13] Flueraru C, Grover CP. Relative measurements of second-order susceptibility with reflective second-harmonic generation. Appl Opt 2003;42:6666–71.
[14] Sekkat Z, Knoll W. Creation of second-order nonlinear optical effects by photoisomerization of polar azo dyes in polymeric films: theoretical study of steady-state and transient properties. J Opt Soc Am B 1995;12:1855–67.
[15] Xu G, Liu XC, Si JH, Ye PX, Li Z, Shen YQ. Modified theory of photoinduced molecular polar alignment in azo polymers. Opt Lett 2000;25:329–31.
[16] Singer KD, Kuzyk MG, Sohn JE. Second-order nonlinear-optical processes in orientationally ordered materials: relationship between molecular and macroscopic properties. J Opt Soc Am B 1987;4:968–76.
[17] Angiolini L, Benelli T, Giorgini L, Mauriello F, Salatelli E. Synthesis of optically active photoresponsive multifunctional polymer containing the side-chain azocarbazole chromophore. Macromol Chem Phys 2006;207:1805–13.
[18] Cho MJ, Choi DH, Sullivan PA, Akelaitis AJP, Dalton LR. Recent progress in second-order nonlinear optical polymers and dendrimers. Prog Polym Sci 2008;33:1013–58.
[19] Pan Q, Fang C, Li F, Zhang Z, Qin Z, Wu X, et al. Thermally stable chromophores for nonlinear optical applications. Mater Res Bull 2002;37:523–31.